Journal of Nonlinear Optical Physics & Materials
Vol. 17, No. 2 (2008) 121–129

World Scientific
www.worldscientific.com

NEW CONCEPTS WITH SURFACE PLASMONS AND NANO-BIOINTERFACES

WOLFGANG KNOLL*, AMAL KASRY, FANG YU, YI WANG,
ANNETTE BRUNSEN and JAKUB DOSTÁLEK

Max Planck Institute for Polymer Research,
Ackermannweg 10, 55128 Mainz, Germany
**knoll@mpip-mainz.mpg.de*

Received 13 May 2008

In classical surface plasmon-based optical biosensors, a surface plasmon mode is resonantly excited on the metallic sensor surface to probe any analyte-binding-induced refractive index changes. The field of the surface plasmon mode evanescently decays from the metal into an adjacent analyte solution with a typical penetration depth of 200 nm. In order to maximize the sensitivity of SPR biosensors, interfacial polymer architectures with binding site densities that considerably exceed planar arrangements through the use of three-dimensional microstructures were introduced. For biosensors based on surface plasmon fluorescence spectroscopy, this type of matrix offers the additional advantage of preventing fluorescence quenching, which is caused by the proximity of the chromophore label to the acceptor states of the noble metal. By means of probing the binding events with long range surface plasmon modes of which field extend much farther into the analyte solution (up to the micrometer range), substantially thicker sensor matrix layers can be used. Into such matrices larger amounts of ligands can be loaded, which enables one to increase the surface density of binding sites and thus to enhance the sensitivity of the biosensor. We present results which show that functionalized hydrogels are very well suited for meeting the demands of these novel biosensor platforms.

Keywords: Surface plasmons; long-range surface plasmons; fluorescence spectroscopy; biointerfaces; hydrogels.

1. Surface Plasmon Fluorescence Spectroscopy

Recently, surface plasmon resonance (SPR) spectroscopy[1,2] has gained enormous popularity as a sensitive optical technique for the investigation of bioaffinity reactions at sensor surfaces.[3] In particular, the introduction of a variety of commercial instruments enabled the use of the SPR technique to spread among the research community, and it has become a routinely used tool in materials research and life science laboratories.

The fundamental setup based on the Kretschmann prism coupling configuration is shown in Fig. 1(a): onto a high-index glass prism a thin Au or Ag film is evaporated, functionalized by an interfacial architecture designed for a specific bioaffinity

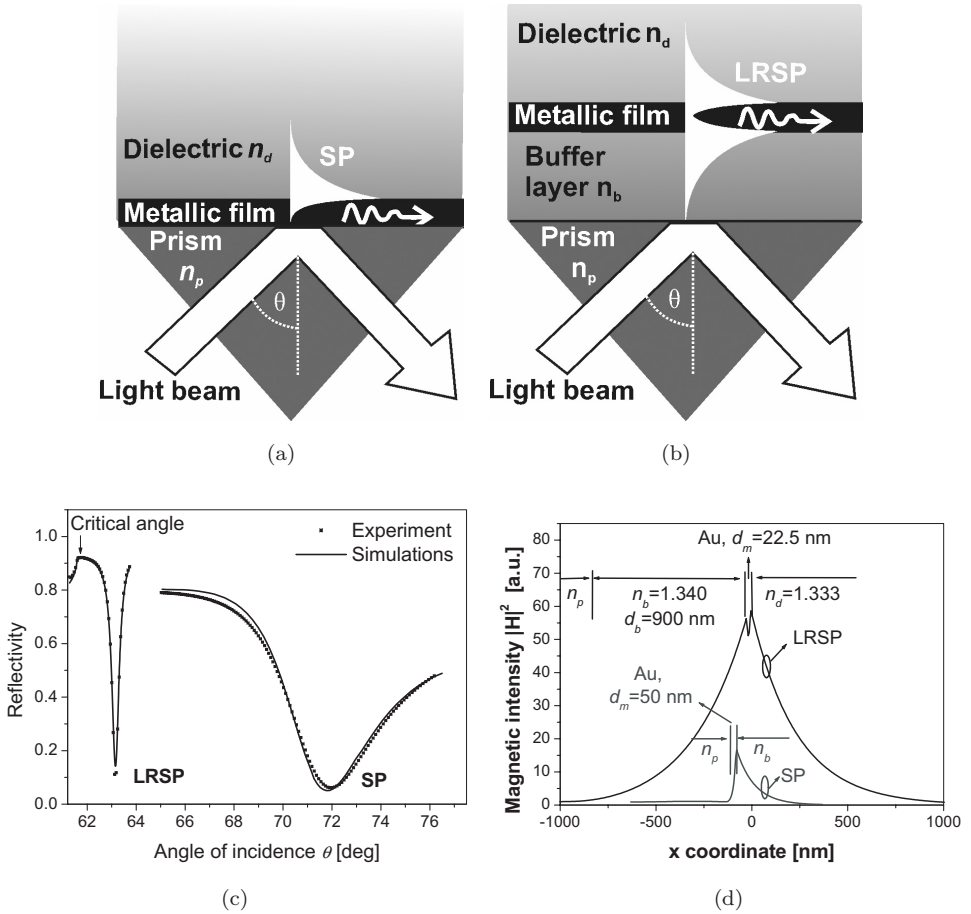

Fig. 1. Kretschmann configuration of the attenuated total internal reflection (ATR) method for the excitation of (a) surface plasmons (SPs) and (b) long-range surface plasmons (LRSPs); (c) comparison of the angular reflectivity spectra measured for the excitation of SPs and LRSPs on a gold film in contact water (parameters indicated in part d); (d) simulated distribution of magnetic intensity across the layer structure upon the excitation of SPs (angle of incidence $\theta = 72°$) and LRSPs (angle of incidence $\theta = 63.1°$) normalized to the intensity of the incident wave in the prism.

reaction, and then brought in direct contact with the aqueous phase of the analyte solution. A laser beam is coupled with the prism and is totally reflected off its base with the metallic coating. At the resonant angle, the laser beam excites surface plasmons on the top metal interface. As seen in Fig. 1(c), the resonant excitation of surface plasmons is manifested as a sharp dip in the angular reflectivity spectrum. Upon resonance, the intensity of the laser beam is compressed to the surface within the surface plasmon mode. The evanescent electromagnetic field of the surface plasmon decays exponentially into the aqueous solution, and for a Au film and the wavelength of 633 nm, the penetration depth (the distance for which the

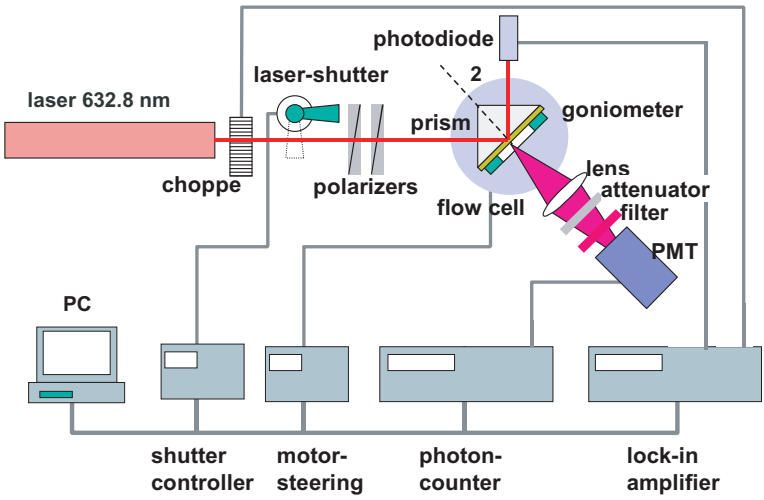

Fig. 2. Experimental setup for the combination of surface plasmon resonance/surface plasmon fluorescence spectroscopy in the Kretschmann configuration.

field amplitude drops to $1/e$) into the aqueous solution is about $L_z = 180\,\text{nm}$; see Fig. 1(d). In plasmon-enhanced fluorescent spectroscopy (SPFS), surface plasmons on the top metal interface are used to excite the captured chromophore-labeled molecules with an increased intensity of the electromagnetic field. The typical setup for the excitation of surface plasmons and the detection of fluorescence-emitted photons is shown in Fig. 2. It comprises a regular instrument for the angular spectroscopy of surface plasmons and a fluorescence detection module consisting of a collection lens, a set of filters specific for the emitted fluorescence photons, and a photomultiplier. It has been shown in a series of investigations that this instrument allows a very sensitive recording of bioaffinity reactions.[4,5] An example is shown in Fig. 3(a): it gives the surface architecture based on a carboxy-dextran brush used to covalently couple the antigens as the recognition sites. The thickness of the swollen brush matches the extent of the evanescent surface plasmon field and prevents the chromophores from being quenched by the proximity to the metal substrate. This way, extreme sensitivities can be achieved.[6] This is documented in Fig. 3(b), showing a series of fluorescence measurements as a function of time after the injection of chromophore-labeled antibody solutions in low concentrations, as indicated. The slope of the linear increase in the fluorescence intensity observed in this mass-transfer-limited regime is plotted in Fig. 3(c) as a function of the bulk concentration, c_0, and is found to be a linear calibration curve covering six orders of magnitude. This extension of SPR spectroscopy with fluorescence detection has been successfully applied to a number of bioaffinity studies of proteins, oligonucleotides or PCR amplicons and, for example, discrimination of single-nucleotide polymorphism (SNP) was possible.[7]

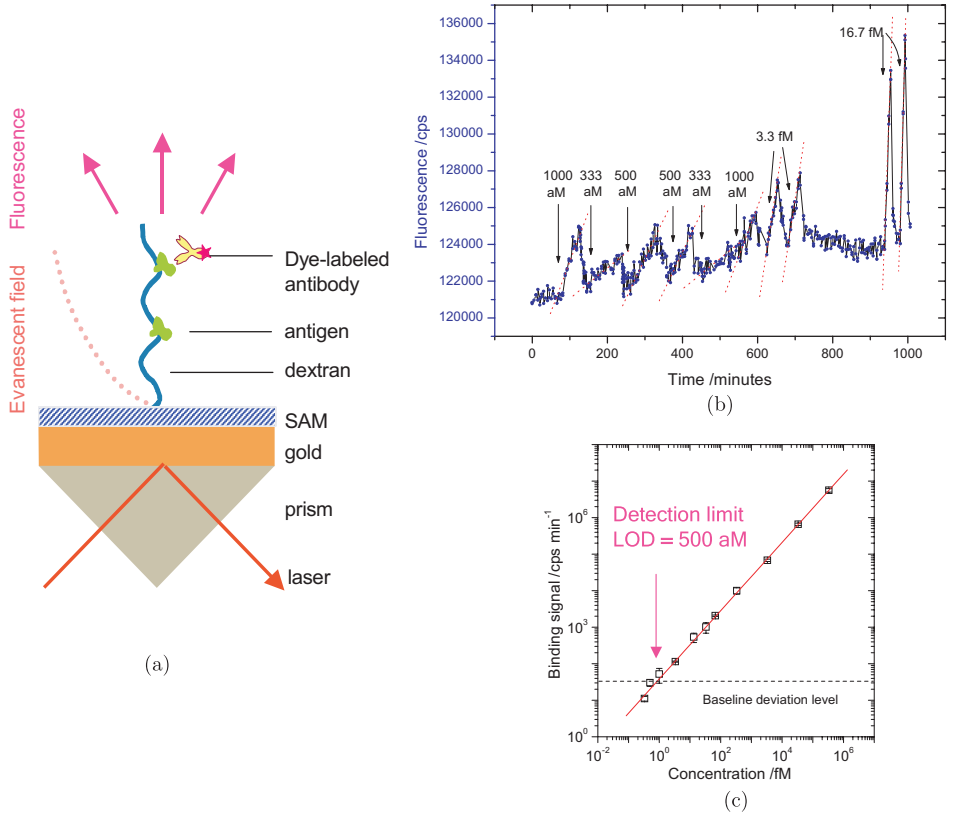

Fig. 3. (Color on line) (a) Interfacial brush architecture with covalently bound antigens, recognized by the dye-labeled antibodies. (b) Fluorescence response upon the injection of antibody solutions of different concentrations (from 333 aM to 16.7 fM, as indicated). Regenerations were performed after every binding recording. (c) Double logarithmic plot of the binding slopes [cf. the dashed lines in (b)] as a function of the injected bulk concentration. The full red line is a fit to these calibration measurements. The dashed line gives the baseline drift stability limit. The intersection of the two lines defines the limit of detection (LOD).

2. Long-Range Surface Plasmon Fluorescence Spectroscopy

A scheme based on the Kretschmann configuration for the excitation of long-range surface plasmons (LRSPs) is given in Fig. 1(b): prior to the noble metal deposition, a cladding layer of a low-refractive-index material ($n \approx 1.33$) is coated onto the prism, thus generating a symmetrical sandwich structure for aqueous samples. The evanescent optical fields of the surface plasmon modes propagating along the two metal/dielectric interfaces with (nearly) identical dispersion properties interact weakly through the metal. Thus, their degeneracy is lifted and two new modes appear: a so-called long-range and a short-range surface plasmon.[8,9] Two features of the LRSP modes are interesting, particularly in connection with fluorescence spectroscopy of analytes bound to the surface matrix (see below). The first advantage

is the extended range of the evanescent field reaching much farther into the buffer solution than normal surface plasmon waves [see Fig. 1(d)], thus allowing the observation of analyte molecules from a much thicker slice of the sensor surface architecture. The second one is the higher intensity of the optical field of the evanescent tail, giving rise to a second mechanism for enhanced fluorescence detection.[10]

An obvious extension of the application of LRSPs for biosensing is their use as the excitation light source for chromophore labels bioconjugated to the analyte molecules and the recording of the emitted fluorescence intensity. Figure 4 gives an example for the potential increase in the emitted intensity by directly comparing the angular dependence of the fluorescence obtained by normal SPFS with that of long-range SPFS: onto the thin Au metal layer (with a Teflon cladding layer between prism and metal in the case of LRSP excitation) another 500 nm of Teflon was spin-coated as an additional spacer layer, followed by solution adsorption of a dye-labeled antibody layer. As one can see, the reflectivity scans in the case of LRSPs show a substantially narrower resonance curve at a much lower angle [in addition, compare with the spectra in Fig. 1(c)].

The peak fluorescence intensity associated with the excitation of the LRSP is 34 times stronger than in the case of normal SPFS. By designing an optimized interfacial matrix, for example, based on the functionalized hydrogels described below, the full potential of these enhancement mechanisms should give rise to more than two orders of magnitude in detection sensitivity for bioaffinity studies.[11]

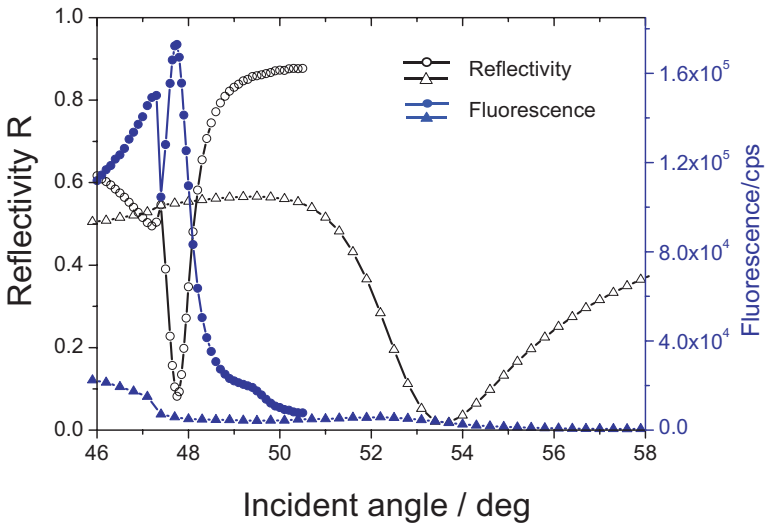

Fig. 4. Comparison of the angular reflectivity scans recorded with normal SPs (open circles) and in the LRSP configuration (open triangles; see also Fig. 1), together with the simultaneously measured angular fluorescence intensity curves (full circles for SP excitation and full triangles for LRSP excitation, respectively). The layer structure consisted of the prism, a 500-nm-thick cladding layer ($n_b = 1.29$) in the case of the LRSP excitation, a Au layer of 40 nm in each case, and the chromophore-labeled protein layer adsorbed from solution.

3. Hydrogels as Binding Matrices for Bioaffinity Studies

The experimental platform that combines the layer architecture required for the excitation of LRSPs and the sensor binding matrix based on an antibody functionalized hydrogel is shown in Fig. 5. The base cladding layer consists of a Teflon polymer material (Cytop from Asahi Inc., Japan; refractive index $n_b = 1.34$) that can simply be spin-coated onto the high-index glass prism, gold film with a thickness of 22.5 nm, which is further functionalized by the hydrogel as the binding matrix. Our strategy for the preparation of highly swollen hydrogels is based on the synthesis of terpolymers incorporating monomers that control the base properties of the resulting hydrogel, such as its hydrophilic/hydrophobic character which influences parameters like the collapse temperature (lower critical solution temperature, LCST), monomers that can be used for the covalent coupling of the binding partners, e.g. antigens or antibodies, or other functional modules like organic dyes or (semiconducting or even magnetic) nanoparticles, and a cross-linking unit which in our case functions through the hydrogen abstraction properties of benzophenon units.[12] After spin-coating this copolymer onto the plasmon guiding metal layer which is preconditioned by a self-assembled monolayer of a benzophenon derivative of a long alkyl chain thiol molecule, the benzophenon moieties are photoactivated by UV light, resulting in a simultaneous cross-linking and grafting of the cross-linked gel to the substrate. Immersion in the buffer solution then leads to the formation of the hydrogel, which can swell to a thickness that exceeds its dry thickness by up to a factor of 10. This means that these matrices are very open structures allowing easy access of the analytes by diffusion from the bulk solution to their stationary partners inside the gel, resulting in a nearly unrestricted affinity binding reaction.

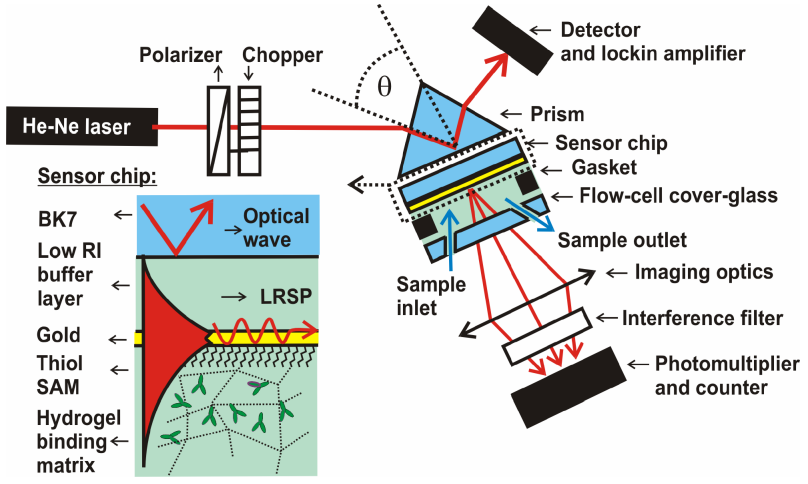

Fig. 5. Schematic of the sensor surface architecture for the excitation of LRSPs in conjunction with a hydrogel as the matrix for the bioaffinity reaction.

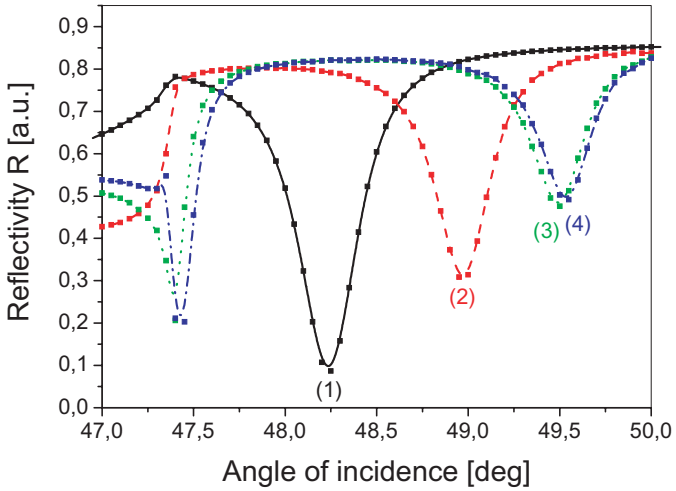

Fig. 6. Measured angular reflectivity spectra for the resonant excitation of LRSPs in a layer structure with an 800 nm Cytop buffer layer and a 22.5-nm-thick gold film: (1) bare gold surface, (2) gold surface with a hydrogel matrix swollen in a HEPES buffer, (3) surface with the gel and the anti-fPSA antibody coupled and (4) after the capture of fPSA.

The functionalization of the swollen gel by the covalent coupling of the affinity partners to the gel matrix depends on a number of factors, including the pH and the ionic strength of the buffer and the isoelectric point of ligands. The example given in Fig. 6 shows the reflectivity spectra recorded for a bare gold surface, a gold surface with the attached dextran-based hydrogel (with a thickness of about 950 nm and a refractive index of $n = 1.348$) and after the immobilization of antibodies against free prostate specific antigen (a-fPSA, from Meridian Life Sciences, Inc.) into the gel. The coupling of the antibody with the dextran-based hydrogel was performed according to the following protocol. First, the carboxyl groups of a modified dextran network were activated by using a 4 min incubation in an aqueous solution with N-hydroxy succinimide (NHS, 0.1 M) and N-(3-dimethylaminopropyl)-N′-ethylcarbodiimide (EDC, 0.4 M). Thereafter, the antibody was bound to the gel from a 10 mM acetate buffer (pH 5) in which a-fPSA antibody was dissolved at the concentration of 100 μg/mL. Finally, the unreacted ester groups were passivated via the introduction of ethanolamine-HCl (1 M).

Figure 7 then documents the first recording of a bioaffinity reaction between fPSA in a solution and the respective antibody a-fPSA immobilized in the gel matrix probed by an LRSP mode. In this experiment, a baseline was first established by flowing the HEPES buffer through the sensor. After that, a series of solutions with the fPSA dissolved at concentrations 0.1, 1, 3 and 10 μg/mL in the HEPES buffer were injected into the flow cell system. The binding of fPSA to the antibodies was observed in real time from induced changes in the reflectivity measured at the angle of incidence $\theta = 49.35°$. The preliminary kinetic analysis of the binding from

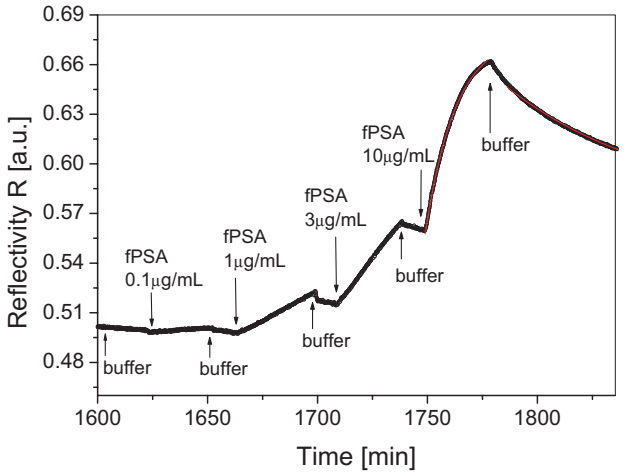

Fig. 7. Sensor response upon the binding of fPSA (injected at different concentrations into the flow cell, as indicated) to antibodies immobilized to the dextran-based hydrogel binding matrix.

a 10 ug/mL fPSA concentration according to

$$R_a(t) = (R_{\max} - R_0)(1 - e^{-(k_a\alpha_0 - k_a)(t-t_0)}) + R_0$$

for the association process and according to

$$R_d(t) = (R_{\max} - R_0)e^{-k_d(t-t_0)} + R_0$$

for the dissociation of the analyte upon injection of the buffer (see Fig. 7) obtained in rate constants $k_a = 4.5 \times 10^3\,\mathrm{M^{-1}\,s^{-1}}$ and $k_d = 2.3 \times 10^{-4}\,\mathrm{s^{-1}}$, respectively, which compare favorably to values reported in the literature for the binding/dissociation of fPSA to a dextran brush ($k_a = 2.2 \times 10^4\,\mathrm{M^{-1}\,s^{-1}}$ and $k_d = 3.2 \times 10^{-4}\,\mathrm{s^{-1}}$.[13]) The reduction of the association rate constant k_a observed for the gel might reflect an osmotic barrier to the diffusion of the analyte into the gel matrix, but needs to be further investigated.

Acknowledgments

Partial funding for this work from the Deutsche Forschungsgemeinschaft (DFG, KN 224/13-1 and Priority Program "Intelligent Hydrogels" KN 224/18-1) and from the EU (FP6-2005-FOOD-036300 "TRACEBACK") is gratefully acknowledged. Furthermore, we thank P. Beines, R. Roskamp, U. Jonas, B. Persson and S. Löfas for helpful discussions.

References

1. H. Räther, *Surface Plasmons* (Springer-Verlag, Berlin, Heidelberg, 1988).
2. W. Knoll, *Ann. Rev. Phys. Chem.* **49** (1998) 569–638.
3. S. Löfas and B. Johnsson, *J. Chem. Soc. Chem. Commun.* **21** (1990) 1526–1528.

4. T. Liebermann and W. Knoll, *Colloid. Surf. A* **171** (2000) 115–130.
5. F. Yu, D. Yao and D. W. Knoll, *Anal. Chem.* **75** (2003) 2610.
6. F. Yu, B. Persson, S. Lofas and W. Knoll, *J. Am. Chem. Soc.* **126** (2004) 8902–8903.
7. W. Knoll, F. Yu, T. Neumann, T. Niu and E. Schmid, Principles and Applications of Surface-Plasmon Field-Enhanced Fluorescence, in *Topics in Fluorescence Spectroscopy*, Vol. 8: Radiative Decay Engineering, eds. J. R. Lakowicz and C. D. Geddes (2005), Chap. 10, pp. 305–332.
8. D. Sarid, *Phys. Rev. Lett.* **47** (1981) 1927–1930.
9. D. Sarid *et al.*, *Appl. Opt.* **21** (1982) 3993–3995.
10. A. Kasry and W. Knoll, *Appl. Phys. Lett.* **89** (2006) 101106.
11. J. Dostalek, A. Kasry and W. Knoll, *Plasmonics* **2** (2007) 97–106.
12. P. W. Beines, I. Klosterkamp, B. Menges, U. Jonas and W. Knoll, *Langmuir* **23** (2007) 2231–2238.
13. F. Yu, B. Persson, S. Lofas and W. Knoll, *Anal. Chem.* **76** (2004) 6765–6770.